Natural Input of Arsenic into a Coral-Reef Ecosystem by Hydrothermal Fluids and Its Removal by Fe(III) Oxyhydroxides

THOMAS PICHLER,* JAN VEIZER, AND GWENDY E. M. HALL†
Ottawa-Carleton Geoscience Centre, University of Ottawa, Ottawa, Ontario, K1N 6N5, Canada

The coral reef that circles Ambitle Island, Papua New Guinea, is exposed to the discharge of a hot, mineralized hydrothermal fluid. The hydrothermal fluids have a pH of ~6 and are slightly reducing and rich in As. Seven individual vents discharge an estimated 1500 g of As per day into an area of approximately 50 × 100 m that has an average depth of 6 m. Despite the amount of As released into the bay, corals, clams, and fish do not show a response to the elevated values. We analyzed hydrothermal precipitates for their chemical and mineralogical composition in order to determine As sinks. Two mechanisms efficiently control and buffer the As concentration: (1) dilution by seawater and (2) incorporation in and adsorption on Fe(III) oxyhydroxides that precipitate when the hydrothermal fluids mix with ambient seawater. Fe(III) oxyhydroxides contain up to 76 000 ppm As, by an order of magnitude the highest As values found in a natural marine environment. Following adsorption, As is successfully retained in the Fe(III) oxyhydroxide deposits because oxidizing conditions prevail and high As activity allows for the formation of discrete As minerals, such as claudetite, arsenic oxide, and scorodite.

Introduction

Arsenic, particularly the reduced form arsenite, is extremely toxic and may cause neurological damage at aqueous concentrations as low as 0.1 mg/L (*1*). In natural waters most of the As is present in inorganic forms, and its mobility is controlled by sorption onto Fe(III) oxyhydroxides, humic substances, and clay minerals (e.g., ref *2*). Sorption of As onto Fe(III) oxyhydroxides, however, does not necessarily imply its permanent removal from solution. Changing redox conditions from oxidizing to reducing, for example, have a great impact on As retention, because As(III) and As(V) have different sorption isotherms with pH (e.g., ref *3*). In addition, the reduction of Fe(III) is a driving factor for release of As because the sorption by Fe(II) minerals is poor. Recrystallization of Fe(III) oxyhydroxide into more thermodynamically stable structures, such as goethite or hematite, is accompanied by a dramatic decrease in specific surface area and, therefore, adsorption capacity (*4*). As a result, As may be released. Whether a net release takes place, however, depends on the amount of As to be incorporated into the crystalline structure of the newly forming mineral (e.g., ref *5*). Several experimental studies have been conducted in order to address the fate and transport of potentially toxic ions (e.g., ref *6*), but there is a need for data and observations from natural systems.

The coral reef in Tutum Bay on the west side of Ambitle Island, Papua New Guinea (Figure 1) is subject to the discharge of hydrothermal fluids from several vent orifices (*7*). Of the potentially toxic trace metals that are released into Tutum Bay only As has a significantly higher concentration than that of seawater (*8*). The hydrothermal fluids contain As concentrations of more than 1000 ppb, and the combined discharge of all vents is estimated to be more than 1500 g of As per day into an area of approximately 50 × 100 m that has an average depth of 6 m. These values are the highest As concentration reported from any marine setting, including black smoker fluids from midocean ridges (e.g., ref *9*).

Coral reefs are sensitive ecosystems where complex interactions of biological, climatic, and oceanographic factors influence reef growth. The most important environmental variables are sea level change, carbonate mineral saturation state, temperature, visible light, ultraviolet light, currents, waves, sedimentation rates, salinity, nutrients, and anthropogenic stresses (*10*). Despite the amount of As released into the bay, corals, clams, and fish do not show a response to the elevated concentrations. Fish have been observed to hover over vent orifices bathing in the hydrothermal fluid. The diversity and health of the coral reef is indistinguishable from reefs that are not exposed to hydrothermal discharge. The skeletons of scleractinian corals and the shells of *Tridacna gigas* clams do not show elevated concentrations of As or other trace metals when compared to specimens collected from outside Tutum Bay (*11*).

The purpose of this work was to determine the role of hydrothermal Fe(III) oxyhydroxide precipitates as a sink for As, to assess their environmental importance, and to compare Tutum Bay deposits to those from nonmarine settings. We employed standard chemical and mineralogical techniques in conjunction with thermodynamic calculations to reconstruct the physicochemical conditions during and after precipitation of Fe(III) oxyhydroxide deposits.

Description of Study Area and Fe(III) Oxyhydroxide Deposits. In Tutum Bay (Figure 1) submarine hydrothermal venting occurs in shallow (5−10 m) water along the inner shelf that contains a patchy distribution of coral-algal reefs surrounded by medium to coarse-grained mixed carbonate-volcaniclastic sand and gravel. Focused discharge of a clear, two-phase fluid occurs from discrete orifices, 10−15 cm in diameter, with phase separation (boiling) at the sea floor. Fluid temperatures at vent orifices are between 89 and 98 °C, and flow rates are estimated to be as high as 300 to 400 L/min. Dispersed or diffuse discharge is present throughout the bay and consists of streams of gas bubbles emerging directly through the sandy to pebbly unconsolidated sediment and through fractures in volcanic rocks. A more detailed description of Tutum Bay can be found elsewhere (*7*), and color photographs are available on a website (http://www.nrcan.gc.ca/~tpichler).

The complete chemical compositions of Tutum Bay hydrothermal fluids have been reported elsewhere (*8*), and the following is a summary of their findings. The composition of the gas is mainly CO_2 (92.6−97.9%) with minor amounts of N_2 (2.2−4.7%), O_2 (0.43−0.73%), CH_4 (0.6−2%), and He (~0.01−0.02%). H_2S was below its detection limit of 0.01%. Compared to seawater the hydrothermal fluids are depleted in Cl, Br, SO_4, Na, K, Ca, Mg, and Sr and enriched in HCO_3,

* Corresponding author phone: (613)231-2601; fax: (613)562-5192; e-mail: tpichler@nrcan.gc.ca.
† Geological Survey of Canada.

10.1021/es980949+ CCC: $18.00
Published on Web 00/00/0000

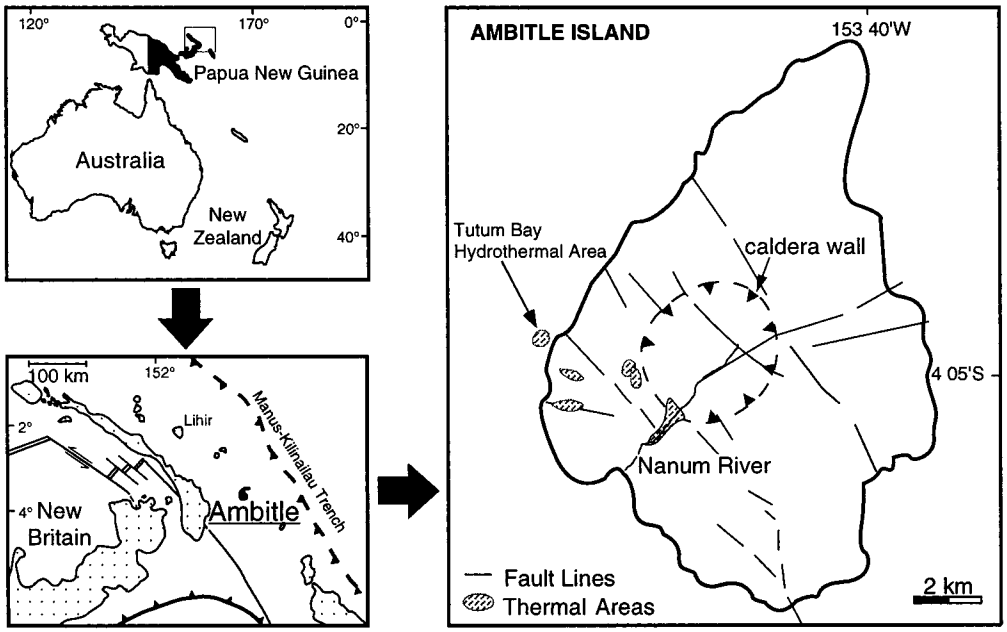

FIGURE 1. Location of Tutum Bay along the west side of Ambitle Island, one of the Feni islands in eastern Papua New Guinea. Geothermal areas indicated in dark are primarily along the western side of the island.

FIGURE 2. Underwater photograph of Tutum Bay vent 1. Field of view is approximately 1 m. White arrows indicate volcanic pebbles, boulders, and fragments of dead corals that are coated with a thin layer of Fe(III) oxyhydroxide (bright yellow to orange). The thickness the Fe(III) oxyhydroxide deposits decreases, stepping away from the point of hydrothermal discharge.

B, Si, Li, Mn, Fe, Rb, Cs, Sb, Tl, and As. All vent fluids had a pH of ~6.1 and Eh of ~ −0.17 v (vent 1 = −0.175 v, vent 2 = −0.171 v, vent 3 = −0.173 v, and vent 4 = −0.175 v). Eh measurements were checked against Quinhydrone solution. These values were also confirmed with the Nernst equation, using the As^{3+}/As^{5+} ratios in Tutum Bay hydrothermal fluids (*8*).

Fe(III) oxyhydroxides are present throughout Tutum Bay where they form as very thin layers on sediment grains in areas of high seafloor temperature. Massive layers and extensive filling of sediment pore space, however, are restricted to the vicinity of vent sites. Here they coat volcanic boulders in bright orange (Figure 2), form distinct bands on coral skeletons, hydrothermal aragonite ($CaCO_3$), and Fe-calcite, and/or precipitate as massive layers in open spaces. They can vary in color from a bright orange to very dark brown (almost black) and in hardness from <1 (talc) to about 2.5 (between gypsum and calcite). Fe(III) oxyhydroxide precipitates were collected at different locations throughout Tutum Bay, using Scuba. A complete listing of all samples and their location relative to vent sites is given in Table 1.

Materials and Methods

Fe(III) oxyhydroxide material was separated from its substrate with a scalpel, rinsed with deionized water to remove halite, and carefully crushed in an agate mortar. Sample powders were dried at room temperature to prevent goethite to hematite conversion (*12*).

Hand specimens, polished thin and thick sections were examined using standard transmitted and reflected light microscopy. Mineral identification was confirmed by scanning electron microscopy (SEM), transmission electron microscopy (TEM), Mössbauer spectroscopy, and powder and single-crystal X-ray diffractometry (XRD). Small sample chips were carbon coated and mounted on aluminum stubs for SEM analysis on a Cambridge Stereoscan 360 scanning electron microscope, fully integrated with an Oxford Instruments (Link) eXL-II energy-dispersive X-ray (EDX) microanalyzer. XRD analyses were performed on a Philips PW 3710, stepping 0.02 °2θ from 2.00° to 88.00 °2θ using copper X-radiation generated at 45 kV and 40 mA.

The chemical composition of Fe(III) oxyhydroxide was determined by microbeam analysis on carbon-coated polished thin sections and by bulk chemical methods on powdered sample material. Electron microprobe analyses were performed on a CAMECA SX-50, operating at 15 kV accelerating voltage, 2 nA beam current and beam diameters varying from <1 to 5 μm. Proton microprobe analyses were carried out on the Ruhr University, Bochum micro-PIXE, on spots of approximately 5 μm diameter, using a 3 MeV beam (*13*), and element concentrations were evaluated with the GUPIX software package (*14, 15*).

Trace element concentrations in Tutum Bay Fe(III) oxyhydroxide deposits were generally low and below the detection limit of conventional microbeam methods. To obtain a more detailed chemical composition of the hydrothermal Fe(III) oxyhydroxide, bulk analyses were carried out on samples FV-1A, FV-1B, V-1B, V-2B I, V-2B II, V-2B III, and V-4.1D. For these samples major elements were obtained by X-ray fluorescence (XRF), and wet chemical methods. As, Au, Br, Hg, Sb, Se, and W were determined by neutron activation analyses (NAA). Ag, Cd, Cs, Hf, In, Mo, Nb, Pb, Rb, Ta, Th, Tl, U, Y, and Zr were determined by inductively coupled plasma mass spectrometry (ICP-MS), and Ba, Be,

TABLE 1. Description of Tutum Bay Hydrothermal Fe Oxyhydroxide Precipitates

sample	location	description	XRD scans
FV-1A	vent 1	massive layers with alternating colors ranging from dark brown to dark orange; indurated and relatively hard compared to the other Fe-oxyhydroxides	protoferrihydrite, gypsum, hematite, As_2O_4, As_2O_5, Fe-smectite, scorodite
FV-1B	vent 1	softer layer of dark orange color from beneath FV-1A	n.d.
V-1B	vent 1	Fe-precipitate on a volcanic boulder	protoferrihydrite
V-2B I	vent 2	massive layer of reddish brown relatively hard Fe-oxyhydroxide that precipitated on dead coral fragments and aragonite	protoferrihydrite, Fe-smectite, claudetite (As_2O_3)
V-2B II	vent 2	soft layer of yellow brown color from beneath V-2B I	protoferrihydrite
V-2B III	vent 2	very thin intermediate layer between V-2B I and V-2B II; may contain significant amounts of both V-2B I and V-2B II	protoferrihydrite
V-4.1D	vent 4	Fe-oxyhydroxide coating volcanic fragments and fragments of dead corals, contains some aragonite	protoferrihydrite
V-2−97	vent 4	very soft orange to orange brown layer on a coral skeleton that fell partly over the vent orifice	protoferrihydrite

Co, Cr, Cu, Ni, Sc, Sr, and V were determined by inductively coupled plasma emission spectrometry (ICP-ES). XRD, XRF, SEM, ICP, and microprobe analyses were carried out at the Geological Survey of Canada, and NAA was performed by Activation Labs in Ancaster, Ontario. Analytical error is as follows: <2% for XRF, <5% for wet chemical analyses, <5% for ICP-ES (except <10% for Ag, Ba and Sr), <10% for ICP-MS, and ~15% for NAA.

Results

Mineralogy. A combination of transmitted light microscopy, XRD, TEM/EDX, and SEM/EDX analyses was applied to clarify the mineralogical history and composition of the Fe(III) oxyhydroxide deposits. Results are listed in Table 1, and representative XRD diffractograms are shown in Figures 3 and 4. Samples with indication of the presence of As-minerals by XRD were further studied by SEM/EDX. Despite the relatively small size of the mineral grains, making identification based on crystal shape difficult, the EDX spectra confirmed their as As-rich nature. The active participation of bacteria in the precipitation of Tutum Bay Fe(III) oxyhydroxides could neither be confirmed nor disproved. Several rounded to subrounded Fe- and Si-rich bodies, approximately 1 μm across, were observed by electron microscopy. Transmission electron microscopic (TEM) analyses, however, did not conclusively confirm the presence of bacteria, although rounded shapes were observed that could be the mineralized remnants of bacteria.

The two diffractograms in Figure 3 represent the two mineralogical endmembers of Tutum Bay deposits. Sample V-2-97 has no distinct peaks, except for two broad humps at approximately 38 and 62° 2θ (d = 2.5 Å and 1.5 Å). These two humps may be groups of adjacent diffuse reflections and indicate the presence of hydrous iron oxide (*16, 17*). Chukhrov et al. (*18*) proposed the name protoferrihydrite for hydrous iron oxides that give only two reflections (2.5 and 1.5 Å) and ferrihydrite for those that give five reflections (2.52, 2.25, 1.97, 1.72, and 1.48 Å). They also concluded that the lesser amount of reflections for protoferrihydrite indicates the initial stage of crystallization. The amorphous nature of many natural Fe(III) oxyhydroxide deposits reflects their very fine grain size and colloidal origin (e.g., ref *19*). Mössbauer spectroscopy confirmed the amorphous nature of any Fe-rich material (mineral) and particle sizes of less than 100 Å for Tutum Bay Fe(III) oxyhydroxides.

Sample FV-1A also shows the two broad humps at approximately 38 and 62° 2θ, but several other sharp peaks are clearly observable (Figure 3b). Mineral identification was aided by SEM/EDX analyses and As_2O_5, scorodite ($FeAsO_4$*$2H_2O$), gypsum, and Fe-smectite could be identified. As_2O_4 and hematite are likely but could not be unequivocally

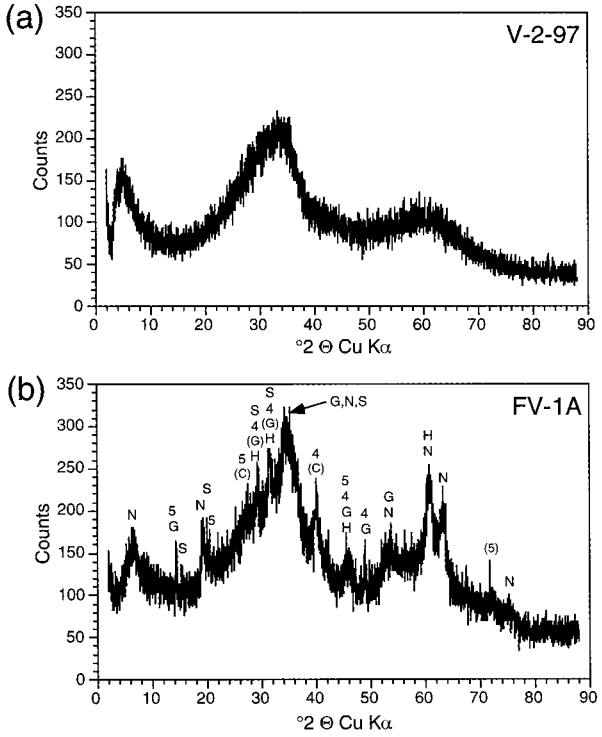

FIGURE 3. Diffractometer patterns for sample V-2-97 (a) and FV-1A (b). The two patterns clearly demonstrate the increasing crystallinity with increasing age. V-2-97 contains only protoferrihydrite, whereas in FV-1A several sharp peaks are superimposed on top of the typical protoferrihydrite pattern: N: smectite (nontronite), G: gypsum, C: claudetite, S: scorodite, H: hematite, 4: As_2O_4, and 5: As_2O_5. Letters in brackets indicate doubtful peaks.

confirmed because they share X-ray reflections with As_2O_5, gypsum, and Fe-smectite (Figure 3b). It was not possible to determine the exact variety of Fe-smectite, but circumstantial evidence points toward nontronite, a dioctahedral Fe-smectite. Nontronite has been found to be the dominant smectite in other Fe(III) oxyhydroxide deposits in submarine settings (e.g., refs *19*−*22*) where the presence of oxygenated seawater either prevents the formation of Fe-rich saponite (Fe^{2+}-smectite) or causes the transformation from saponite to nontronite (*23*). The presence of kankite ($FeAsO_4$*$3.5H_2O$), hydrogenarsenate ($H_5As_3O_{10}$), and/or hydrated hydrogenarsenate ($H_3As_4O_4$*$3H_2O$) is possible but could not be unambiguously confirmed by XRD or SEM/EDX.

The outer layer of sample V-2B (V-2B I, Table 1, and Figure 4a) represents a mineralogical composition intermediate between the two samples in Figure 3 (V-2-97 and FV-1A).

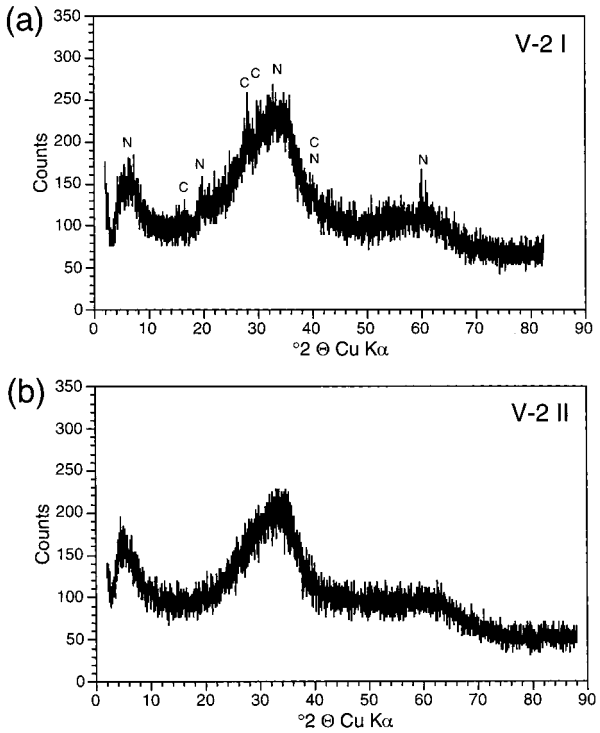

FIGURE 4. Diffractometer patterns for sample V-2 II (a) and V-2 I (b). The two patterns clearly demonstrate the importance of seawater contact during aging. The sample V-2 I, although slightly younger than V-2 II, is more crystalline because it remained in contact with either seawater or a mixture of seawater and vent fluid (seawater ≫ vent fluid). C: claudetite, N: smectite (nontronite).

Here the presence of an Fe-smectite and claudetite (As_2O_3) could be confirmed. The reflections are not as strong as those for the same mineral in sample FV-1A which may indicate either a lesser amount of mineral present or poorer crystallinity. Claudetite was not conclusively observed in sample FV-1A. The reflections for Fe-smectite and claudetite are absent in the softer and lighter colored material of sample V-2 II that was collected from beneath V-2 I. This scan is almost identical to that of V-2-97.

Chemistry. Tutum Bay Fe(III) oxyhydroxide deposits are almost identical in their chemical composition, and the average composition ($n = 7$) is as follows: SiO_2 (15.3%), TiO_2 (0.1%), Al_2O_3 (1.0%), $Fe_2O_3{}^T$ (50.0%), MnO (0.1%), MgO (0.9%), CaO (2.8%), Na_2O (0.8%), K_2O (0.2%), P_2O_5 (0.2%), $CO_2{}^T$ (2.0%), S^T (0.04%), Ag (1 ppm), Au (210, ppb), As (55000 ppm), Ba (130 ppm), Be (38 ppm), Br (11 ppm), Co (9 ppm), Cr (30 ppm), Cs (2.4 ppm), Cu (40 ppm), Ga (1.4 ppm), Hf (0 ppm), Hg (<5 ppm), In (0.1 ppm), Mo (1.4 ppm), Nb (18 ppm), Ni (0.3 ppm), Pb (23 ppm), Rb (6.5 ppm), Sb (200 ppm), Sc (1.4 ppm), Se (<11 ppm), Sr (990 ppm), Th (0.1 ppm), Tl (2.1 ppm), U (0.7 ppm), V (33 ppm), W (<12 ppm), Y (14 ppm), Zn (38 ppm), and Zr (2.1 ppm). Mössbauer spectroscopic analyses of samples FV-1 and V-2 confirmed that iron is exclusively present in its trivalent state. Despite the absence of quartz, elevated SiO_2 concentrations of up to 20% are common in marine Fe(III) oxyhydroxides (e.g., ref *19*).

Elements that are usually enriched in Fe(III) oxyhydroxides such as Co and V are below crustal abundance and well below their typical concentrations in volcanic rocks from island-arc settings. Arsenic, on the other hand, is 2 orders of magnitude higher than expected and clearly sets Tutum Bay Fe(III) oxyhydroxides apart from other submarine deposits (e.g., ref *24*). Values are as high as 62 000 ppm by NAA (Table 1, Supporting Information) and 76 000 ppm by proton probe analysis (Table 2, Supporting Information). The discrepancy

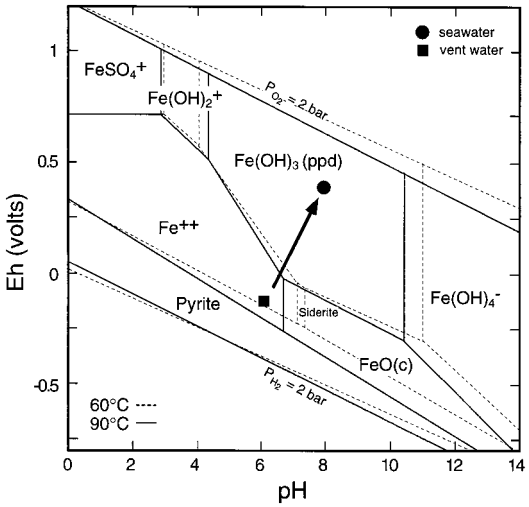

FIGURE 5. Eh-pH diagram for the system Fe−O−H−SO_4−HCO_3 at 60 °C (dashed lines) and 90 °C (solid lines) at a pressure of 2.026 bar. Activities of Fe, SO_4, and HCO_3 are assumed to be 10^{-5}, 10^{-3}, and 10^{-3}, respectively. $Fe(OH)_3$(ppd) is the field of amorphous Fe(III) oxyhydroxide. The arrow indicates the mixing trend between hydrothermal fluid and seawater.

between the two values is a result of different analytical methods. The NAA was carried out on bulk samples, and values reflect average sample concentrations. Although values scatter significantly, considering the relatively high analytical uncertainty of this method (~15%), the samples can be regarded as being within the same concentration range (Table 1, Supporting Information). The As concentrations determined by proton probe, on the other hand, represent only a very small sample area, and values scatter well beyond their maximum analytical error of <5%. This observation is in accord with the heterogeneous nature of Tutum Bay Fe-(III) oxyhydroxide deposits. Proton probe analyses of differently colored layers in sample FV-1A revealed that darker layers generally have higher As concentrations, but there is no definite interelement correlation (Table 2, Supporting Information).

Discussion

Weathering of Fe-bearing minerals and direct precipitation from solution are the two processes that lead to the formation of Fe(III) oxyhydroxides, such as goethite, lepidocrocite, hematite, and ferrihydrite (e.g., refs *18−20, 22, 24, 25−28*). In Tutum Bay vent fluids (Eh ~ −0.17 V and pH ~ 6.1) Fe^{3+} is effectively absent and as a result precipitation has to proceed via oxidation of Fe^{2+}. This is easily achieved through mixing with oxygenated seawater (e.g., ref *29*) and results in an increase of Eh and pH and a decrease in temperature, all of which favor the precipitation of Fe(III) oxyhydroxide (Figure 5). At the same time conditions are not oxidizing enough to cause precipitation of an As-rich mineral directly from the hydrothermal solution (Figure 6).

The degree of crystallinity as deduced from XRD analyses seems to be directly related to (a) the age of the precipitate and (b) exposure to seawater. Samples FV-1A and V-2 I, older than V-1B, V-2−97, and V-4.1D, clearly show the more complex XRD patterns. These two samples are the outer layers of their respective Fe(III) oxyhydroxide deposits and were exposed to a mixture of seawater and hydrothermal fluid (seawater ≫ hydrothermal fluid) at the time of sampling. The two samples, FV-1B and V-2 II, collected from layers just beneath FV-1A and V-2 I, were not directly exposed to seawater and contain only protoferrihydrite.

The first As phase to appear in the XRD patterns of Tutum Bay Fe(III) oxyhydroxide deposits is claudetite (As_2O_3), a

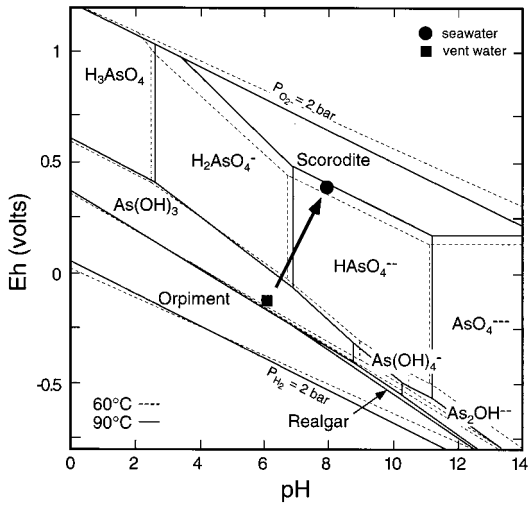

FIGURE 6. Eh-pH diagram for the system As−Fe−O−H−SO_4−HCO_3 at 60 °C (dashed lines) and 90 °C (solid lines) at a pressure of 2.026 bar. Activities of As, Fe, SO_4, and HCO_3 are assumed to be 10^{-6}, 10^{-5}, 10^{-3}, and 10^{-3}, respectively. The arrow indicates the mixing trend in Eh-pH space between hydrothermal fluid and seawater. At Tutum Bay vent fluid concentrations arsenic remains in solution except for very oxidizing conditions. The conditions necessary for the formation of scorodite, however, cannot be achieved by mixing the hydrothermal fluid with seawater, because respective Fe and As concentrations would be too low.

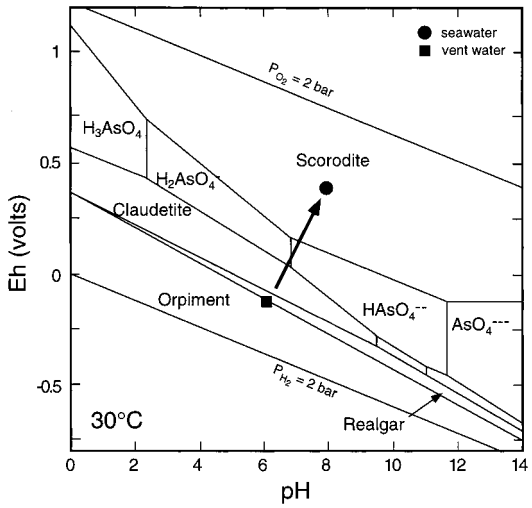

FIGURE 7. Eh-pH diagram for the system As−Fe−O−H−SO_4−HCO_3 at 30 °C (ambient seawater temperature) at a pressure of 2.026 bar and very high As concentration. Activities of As, Fe, SO_4, and HCO_3 are assumed to be $10^{-0.8}$, 10^{-5}, 10^{-3}, and 10^{-3}, respectively. At such high activity of As, the stability field for $As(OH)_3$ is replaced by claudetite, and the field for scorodite increases drastically.

trivalent arsenic oxide. Claudetite is stable only at extremely high arsenic activity ($[As^{3+}] > 10^{-0.8}$ at 25 °C) (Figure 7) which was not present at the time of precipitation of the Fe(III) oxyhydroxide (Figure 6). Arsenic compounds are generally quite soluble, and, as a result, postdepositional interaction with seawater or very dilute hydrothermal fluid should cause the formation of claudetite via dissolution and recrystallization. This process is thought to be analogous to the formation of goethite and/or hematite from amorphous Fe(III) oxyhydroxide (e.g., refs *18* and *25*). High As activity and increasing oxidizing conditions cause a transformation of claudetite into pentavalent arsenic oxide (As_2O_5) and scorodite, the next minerals to appear in the XRD pattern of sample FV-1A (Figures 3b and 7). Additionally, As may be incorporated into structural sites during conversion of ferrihydrite into more crystalline forms, such as goethite and/or hematite (e.g., ref *6*).

The Chemical Composition of Tutum Bay Fe(III) Oxyhydroxides. Scavenging of elements into and onto metal hydroxides is a result of coprecipitation, adsorption, surface complex formation, ion exchange, and penetration of the crystal lattice (*28*). In natural systems it is often impossible to distinguish between coprecipitation and adsorption (*30*). Adsorption, however, has been observed to be the basis of most surface-chemical reactions (*3*) making it the most likely cause for the minor and trace element composition in Tutum Bay Fe(III) oxyhydroxides. With the exception of As, trace element concentrations are low and reflect their low concentrations in the hydrothermal fluid (*8*).

The oxidation, speciation, and solubility of As compounds are largely controlled by inorganic processes (e.g., ref *31*). However, microbial oxidation and reduction are possible despite the fact that As is lethal to microorganisms (*32*−*34*). Arsenic compounds exhibit a strong affinity toward adsorption onto and/or coprecipitation with iron hydroxides. The adsorption of As onto iron hydroxides is controlled by its oxidation state (As(III) vs As(V)) and the specific surface area of the adsorbent, which in turn is directly related to its mineralogy and decreases in the order ferrihydrite > goethite > lepidocrocite > hematite (*35*). Several experimental studies have found that As(III) adsorption at standard conditions (25 °C, 1 bar) is generally rapid and strongest at a pH of approximately 6−7 (e.g., refs *35*−*37*). Comparing these experimental conditions with those present in Tutum Bay it is not surprising that here As concentrations are exceedingly high in Fe(III) oxyhydroxides. The strong pH control would also explain the relatively low As concentration in deep sea Fe(III) oxyhydroxide deposits, where hydrothermal solutions have a significantly lower pH than Tutum Bay vent fluids. Mixing between seawater and hydrothermal fluid, therefore, would have to be extremely high in order to reach a pH that is favorable for extensive As adsorption. Thus preventing precipitation because of its low concentration in seawater As becomes too diluted in the mixture.

The concentration of As in Tutum Bay Fe(III) oxyhydroxide deposits is actually so high that it cannot be considered a trace element. Following Fe and Si, As is the third most abundant element, and concentrations are the highest reported from any marine setting, illustrating the special nature of the Tutum Bay hydrothermal system. Arsenic concentrations in Tutum Bay vent fluids are also the highest reported from a submarine setting (*9*). This clearly sets Tutum Bay apart from deep sea hydrothermal systems and underlines its close relationship to onland hydrothermal systems. In onland systems, As is a common constituent of hydrothermal fluids and hydrothermal precipitates, with concentrations in silica sinters of up to 88 000 ppm (*38*). The highest As concentrations, however, are found in Fe(III) oxyhydroxide deposits in stream beds and/or soils associated with mine drainage, where concentrations of up to 120 000 ppm have been reported (*34*). The strong affinity between Fe(III) oxyhydroxides and As is a blessing in such an environment because As is readily removed from solution and stored (e.g. ref *37*). If Fe(III) oxyhydroxide deposition takes place in streams, the concentration of As in solution decreases exponentially, and removal is complete after a few kilometers downstream from the point of contamination (*34, 39*).

In Tutum Bay, Fe(III) oxyhydroxide also seems to successfully reduce the input of As into seawater, thus preventing the certain collapse of the surrounding coral reef ecosystem. Compared to the situation onland, As removal in Tutum Bay is perpetual because here the conditions remain oxidizing at all times due to continuous flushing and renewal of seawater. In onland settings, in particular in soils and small streams, reducing conditions are common and promote the

stability of As(III) and Fe(II) in place of As(V) and Fe(III). This leads to lower sorption (retention) and greater leaching of As (e.g., ref *35*). In onland systems, additional transformation of As(V) to As(III) under slightly reducing conditions can also be microbially mediated. Ahmann et al. (*32*) reported the discovery of a microorganism that gains energy for growth from reduction of As(V) to As(III) in the absence of oxygen. Insufficient activity of As during aging of an Fe(III) oxyhydroxide may also prevent the formation of discrete As-minerals (Figures 6 and 7). As a result, As is released into solution, because recrystallization of an amorphous material drastically reduces the specific surface area and, therefore, its capacity to adsorb ions (e.g., ref *4*).

We identified hydrothermal Fe(III) oxyhydroxide deposits as the sink for the high As concentrations released into Tutum Bay, and our results indicate that the conditions are ideal for the removal of As from the hydrothermal fluids. Removal from the hydrothermal fluid is most likely complete, although As is initially present as As(III), which is more reactive, more soluble, and less adsorbed onto Fe(III) oxyhydroxide surfaces than As(V) (e.g., ref *35*). Mixing between hydrothermal fluids and seawater causes rapid oxidation of Fe(II) and, therefore, the precipitation of protoferrihydrite in favor of more crystalline Fe(III) oxyhydroxides. At that time As remains in its trivalent state, because its oxidation process is slower than that of Fe(II). Protoferrihydrite and ferrihydrite are the strongest As adsorbents among the Fe(III) oxyhydroxides (*35*) and their maximum sorption of As(III) is at a pH of approximately 7 (*37*). Mixing between seawater (pH = 8) and the hydrothermal fluid (pH = 6.1) increases the pH toward 7.

After precipitation and adsorption, aging in contact with seawater and, therefore, under oxidizing conditions causes recrystallization of protoferrihydrite and the neo-formation of nontronite, gypsum, and various As-minerals. Through time, arsenic is successfully retained in the Fe(III) oxyhydroxide deposits, because oxidizing conditions prevail and the high As concentration allows for the formation of discrete As minerals, such as claudetite, arsenic oxide, and scorodite.

Acknowledgments

Most of this research was funded by an American Chemical Society, Petroleum Research Grant (No. 31585-AC8) and Natural Sciences and Engineering Research Council of Canada operating grant to Jan Veizer. Thomas Pichler acknowledges the support of two Geological Society of America, Student Research Grants (No. 5681-95 and 5904-96). Dr. Denis Rancourt, University of Ottawa, is thanked for the Mössbauer analyses. Dr. Danielle Fortin, University of Ottawa, is thanked for help with the TEM analyses. An earlier version of this manuscript benefited from comments by Dr. Matthew Leybourne, Geological Survey of Canada.

Supporting Information Available

Tables 1 and 2 of major, minor, and trace element composition of Tutum Bay hydrothermal Fe(III) oxyhydroxide precipitates and proton probe traverse across differently colored layers in Fe(III) oxyhydroxide. This material is available free of charge via the Internet at http://pubs.acs.org.

Literature Cited

(1) *1*)WHO, *Guidelines for drinking-water quality*; World Health Organization: Geneva, 1993.
(2) Mok, W. M.; Wai, C. M. In *Arsenic in the environment, Part 1: Cycling and Characterization*; Nriagu, J. O., Ed; Wiley: New York, 1994; pp 99−118.
(3) Stumm, W.; Morgan, J. J. *Aquatic Chemistry*, 3rd ed.; Wiley-Interscience: New York, 1996; p 1022.
(4) Morgan, J. J.; Stumm, W. *J. Colloid Interface Sci.* **1964**, *9*, 347−359.
(5) Spadini, L.; Manceau, A.; Schindler, R. W.; Charlet, L. *J. Colloid Interface Sci.* **1994**, *168*, 73−86.
(6) Ford, R. G.; Bertsch, P. M.; Farley, K. J. *Environ. Sci. Technol.* **1997**, *31*, 2028−2033.
(7) Pichler, T.; Dix, G. R. *Geology* **1996**, *20*, 435−438.
(8) Pichler, T.; Veizer, J.; Hall, G. E. M. *Mar. Chem*. In press.
(9) Von Damm, K. L. In *Seafloor hydrothermal systems*; S. E. Humphries, et al., Eds.; American Geophysical Union, 1995; Geophysical Monograph 91, pp 222−247.
(10) Smith, S. V.; Buddemeier, R. W. *Annu. Rev. Ecol. Systematics* **1992**, 23, 89−118.
(11) Pichler, T. Ph.D. Dissertation, Univerity of Ottawa, Ottawa, Canada, 1998.
(12) Deer, W. A.; Howie, R. A.; Zussmann, J. *An Introduction to the Rock-Forming Minerals*, 2nd ed.; Longman Scientific & Technical: Essex, 1992; p 696.
(13) Bruhn, F.; Bruckschen, P.; Richter, D. K.; Meijer, J.; Stephan, A.; Veizer, J. *Nucl. Instr. Methods Phys. Res.* **1995**, *104*, 409−414.
(14) Maxwell, J. A.; Teesdale, W. J.; Campbell, J. L. *Nucl. Instr. Methods Phys. Res.* **1995**, *B95*, 407−421.
(15) Maxwell, J. A.; Teesdale, W. J.; Campbell, J. L. *Nucl. Instr. Methods Phys. Res.* **1989**, *B43*, 218−230.
(16) Towe, K. M.; Bradley, W. F. *J. Colloid Interface Sci.* **1967**, *24*, 384−392.
(17) Giessen, A. A. *J. Inorg. Nucl. Chem*. **1966**, *28*.
(18) Chukhrov, F. V.; Groshkov, A. I.; Zirijagin, B. B.; Yermilova, L. P.; Balashova, V. V. *Intern. Geol. Rev.* **1973**, *16*, 1131−1143.
(19) Puteanus, D.; Glasby, G. P.; Stoffers, P.; Kunzendorf, H. *Mar. Geol.* **1991**, *98*, 389−409.
(20) Alt, J. C. *Mar. Geol.* **1988**, *81*, 227−239.
(21) Stoffers, P.; Singer, A.; McMurtry, G. M.; Arquit, A.; Yeh, H.-W. *Geol. Jahrb.* **1990**, *D92*, 615−628.
(22) Hekinian, R.; Hoffert, M.; Larqué, P.; Chemineé, J.-L.; Stoffers, P.; Bideau, D. *Econ. Geol.* **1993**, *88*, 2099−2121.
(23) Andrews, A. J. *Contr. Min. Petrol.* **1980**, *73*, 323−340.
(24) Stoffers, P.; Glasby, G. P.; Stüben, D.; Renner, R. M.; Pierre, T. G.; Webb, J.; Cardile, C. M. *Mar. Geores. Geotechnol.* **1993**, *11*, 45−86.
(25) Schwertmann, U.; Fischer, R. W. *Geoderma* **1973**, *10*, 237−247.
(26) Murray, J. W. In *Marine Minerals*; Burns, R. G., Ed.; Mineralogical Society of America: Washington, 1979; Vol. *6*, pp 47−98.
(27) Fortin, D.; Leppard, G. G.; Tessier, A. *Geochim. Cosmochim. Acta* **1993**, *57*, 4391−4404.
(28) Chao, T. T.; Theobald, J. P. K. *Econ. Geol.* **1976**, *71*, 1560−1569.
(29) Millero, F. J.; Sotolongo, S.; Izaguirre, M. *Geochim. Cosmochim. Acta* **1987**, *51*, 793−801.
(30) Drever, J. I. *The Geochemistry of Natural Waters*; Prentice Hall: Englewood Cliffs, 1988; p 392.
(31) O'Neill, P. In *Heavy metals in soils*; Pacey G. E., Ford J. A., Eds.; Blackie: Glasgow, 1990; pp 83−99.
(32) Ahmann, D.; Roberts, A. L.; Krumholz, L. R.; Morel, F. M. M. *Nature* **1994**, *371*, 750.
(33) Baldi, F. In *Chemistry of aquatic systems; local and global perspectives.*; Bidoglio G., Stumm W., Eds.; Kluwer Academic Publishers: Dordrecht − Boston−London, Netherlands, 1994; Vol. *5*, pp 121−152.
(34) Leblanc, M.; Achard, B.; Othmann, D. B.; Luck, J. M.; Bertand-Sarfati, J.; Personne, J. C. *Appl. Geochem*. **1996**, *11*, 541−554.
(35) Bowell, R. J. *Appl. Geochem*. **1994**, *9*, 279−286.
(36) Manning, B. A.; Goldberg, S. *Environ. Sci. Technol.* **1997**, *31*, 2005−2011.
(37) Pierce, M. L.; Moore, C. B. *Environ. Sci. Technol.* **1980**, *14*, 214−216.
(38) Seward, T. M.; Sheppard, D. S. In *Guide to active epithermal (geothermal) systems and precious metal deposits of New Zealand*; Henley R. W., et al., Eds.; Gebrueder Borntraeger: Berlin, 1986; pp 81−91.
(39) Davis, J. A.; Fuller, C. C.; Rea, B. A.; Claypool-Frey, R. G. In *Water-Rock Interaction*; Balkema: Rotterdam, 1989; pp 187−189.

Received for review September 14, 1998. Revised manuscript received January 22, 1999. Accepted February 1, 1999.

ES980949+